Photometric study of open clusters Berkeley 96, Berkeley 97, King 12, NGC 7261, NGC 7296, and NGC 7788

Mon. Not. R. Astron. Soc. **000**, 1–?? (2013) Printed 5 September 2018 (MN LATEX style file v2.2)

Photometric study of open clusters Berkeley 96, Berkeley 97, King 12, NGC 7261, NGC 7296, and NGC 7788

E.V. Glushkova,[1,2⋆] M.V. Zabolotskikh,[2] S.E. Koposov,[2,3] O.I. Spiridonova,[4] S.I. Leonova,[2] V.V. Vlasyuk [4], and A.S. Rastorguev[1,2]

[1] *Faculty of Physics, Lomonosov Moscow State University, Moscow, 119992 Russia*
[2] *Sternberg Astronomical Institute, Lomonosov Moscow State University, Universitetsky pr. 13, Moscow, 119992 Russia*
[3] *Institute of Astronomy, University of Cambridge, Madingley Road, Cambridge, CB3 0HA UK*
[4] *Special Astrophysical Observatory, Russian Academy of Sciences, Nizhnii Arkhyz, Karachai-Cherkessian Republic, 357147 Russia*

Accepted 2012 December 00. Received 2012 December 00; in original form 2012 December 00

ABSTRACT

We present BVR_cI_c CCD photometry in the fields of six Galactic open clusters toward the Perseus spiral arm. These data, complemented with J, H, and K_S magnitudes from 2MASS, have been used to determine the ages, distances, and colour excesses $E(B-V)$ for these clusters: 40 Myr, 3180^{+440}_{-380} pc, 0.54 ± 0.03 mag (Berkeley 96); 250 Myr, 2410^{+220}_{-200} pc, 0.77 ± 0.06 mag (Berkeley 97); 70 Myr, 2490^{+180}_{-170} pc, 0.51 ± 0.05 mag (King 12); 160 Myr, 2830^{+160}_{-150} pc, 0.88 ± 0.09 mag (NGC 7261); 280 Myr, 2450^{+190}_{-170} pc, 0.24 ± 0.03 mag (NGC 7296); and 160 Myr, 2750^{+220}_{-210} pc, 0.49 ± 0.02 mag (NGC 7788). We found gaps in the mass function of clusters Be 97, King 12, and NGC 7788 in the mass intervals of [1.3–1.5], [1.4–1.6], and [1.5–1.7] solar masses, respectively.

Key words: Galaxy: open clusters and associations: individual: Berkeley 96, Berkeley 97, King 12, NGC 7261, NGC 7296, and NGC 7788

1 INTRODUCTION

Despite important progress in the study of the structure and evolution of the Galactic disk, many questions remain unanswered, such as the location of inner spiral arms or determination of the corotation distance. Open star clusters (OCLs) play the most important role in the investigation of Galactic disk properties, because their ages, distances, and colour excesses can be easily evaluated from photometric CCD observations. However, the number of investigated OCLs with the heliocentric distances above 2 kpc is still small. We developed and carry out a program of investigation of the Perseus spiral arm based on the space and age distributions of open clusters. We already obtained BVRI CCD photometry and estimated the main physical parameters of six OCLs in this region: King 13, King 18, King 19, King 20, NGC 136, and NGC 7245 (Glushkova et al. (2010)).

This study is concerned with another sample of six open clusters located toward the Perseus spiral arm: Berkeley 96 ($l = 103\overset{\circ}{.}72$, $b = -2\overset{\circ}{.}09$), Berkeley 97 ($l = 106\overset{\circ}{.}66$, $b = 0\overset{\circ}{.}38$), King 12 ($l = 116\overset{\circ}{.}12$, $b = -0\overset{\circ}{.}13$), NGC 7261 ($l = 104\overset{\circ}{.}04$, $b = 0\overset{\circ}{.}91$), NGC 7296 ($l = 101\overset{\circ}{.}88$, $b = -4\overset{\circ}{.}60$), and NGC 7788 ($l = 116\overset{\circ}{.}43$, $b = -0\overset{\circ}{.}78$).

The WEBDA database on open star clusters [1] contains the following information on photometry of the clusters under study.

Berkeley 96. Del Rio (1984) measured photoelectric UBV magnitudes of 10 stars and derived the cluster distance $r = 5.3$ kpc and the colour excesses $E(B-V) = 0.68$ and $E(U-B) = 0.50$ mag.

Berkeley 97. Tadross (2008) evaluated the distance to the cluster $r = 1.8$ kpc, its age $t \approx 200$ Myr, and colour excess $E(B-V) = 0.75$ mag, using JHK_s magnitudes from 2MASS Point Source Catalog (Skrutskie et al. 2006) exclusively.

King 12. Mohan & Pandey (1984) obtained photoelectric UBV magnitudes for 30 stars and found the cluster distance to be $r = 2.49$ kpc and its colour excess $E(B-V)$ to vary from 0.52 to 0.69 mag (differential reddening). Haug (1970) measured photoelectric UBV magnitudes of four stars in the cluster field.

NGC 7261. Based on UBV photographic magnitudes of 147 stars, Fenkart (1968) determined the cluster age $t \approx 10$ Myr, distance $r = 3230$ pc, and colour excesses $E(B-V) = 1.00$ and $E(U-B) = 0.73$ mag. Using $UBViyz$ photoelectric photometry of five K-giants, Jennens & Helfer

⋆ E-mail: elena@sai.msu.ru

[1] http://www.univie.ac.at/webda

(1975) found the cluster age $t \approx 200$ Myr, distance $r = 2200$ pc, metal abundance $[Fe/H] = -0.7$, and colour excess $E(B-V) = 0.48$ mag. Hoag et al. (1961) obtained photoelectric UBV photometry for 28 stars and photographic UBV photometry for 53 stars; Eggen (1968) measured UBV photoelectric magnitudes for two stars; Kubinec (1973) measured photographic BV magnitudes for seven stars.

NGC 7296. Based on Δa and BVR CCD photometry for about 140 stars, Netopil et al. (2005) determined the cluster age $t \approx 100$ Myr, distance $r = 2930$ pc, and colour excesses $E(B-V) = 0.15 \pm 0.02$ and $E(V-R) = 0.00 \pm 0.02$ mag.

NGC 7788. Haug (1970) measured photoelectric UBV magnitudes of five stars; Becker (1965) measured photographic UBV magnitudes of 113 stars; and Frolov (1977) found photographic BV magnitudes of 67 stars.

The clusters Be 96, King 12, NGC 7261, and NGC 7788 were studied by means of photographic and photoelectric photometry down to V-band limiting magnitudes of 14.5–16.5 mag. According to the estimates reported by the above authors and by Dias et al. (2002) for NGC 7788, the distances to all these clusters exceed 2 kpc. Hence the published colour-magnitude diagram (CMD) isochrone fits involved only the upper parts of the main sequences of the clusters studied whose physical parameters could therefore be determined with large errors. Berkeley 97 was studied using only JHK_S data, also down to a shallow limiting magnitude. The only published color-magnitude diagram of NGC 7296 is based on CCD photometry and goes down to a V-band limiting magnitude of 16.8 mag. CCD data is known to be often fraught with systematic errors and we therefore decided to repeat the observations of this cluster. We also wanted to verify a very small value $E(V-R) = 0.00$ derived by Netopil et al. (2005). All these factors justify our choice of the six open clusters listed above.

2 OBSERVATIONS AND DATA REDUCTION

We observed six open clusters in the Johnson/Kron–Cousins broadband BVR_cI_c using the Zeiss–1000 telescope at the Special Astrophysical Observatory of the Russian Academy of Sciences equipped with a photometer based on an EEV 42–40 2K × 2K CCD. The pixel size, readout noise, and gain were equal to 13.5 μm, $4e^-$, and $2.08e^-$ per ADU, respectively. The scale and field of view were equal to $0\farcs207$/pixel and about $7'$, and $0\farcs238$/pixel and about $8'$ during the 2003 and 2009 observations, respectively. The scale and field of view size differences were due to changed photometer layout. Table 1 shows the log of observations. Its columns contain dates of observation, object names, air masses $X = \sec z$, and exposure times in each band. Figure 1 shows the images of all six clusters under study taken in V–band with the exposure 300 s with the limiting magnitude of about 21 mag.

Primary data processing, image extraction, and analysis were performed in the standard way using the ESO-MIDAS environment and the DAOPHOT/ALLSTAR program package (Stetson 1987). Prior to the data reduction, we transformed the pixel coordinates for every star into celestial coordinates for the epoch J2000. In addition to the program clusters studied, the open cluster NGC 7790 was observed several times for each night as a photometric standard, and the NGC 6940 cluster was used once as a photometric standard (see Table 1). The standard magnitudes for stars in the fields of NGC 7790 and NGC 6940 were taken from Stetson's database [2]. The ranges of magnitudes and colours for about 250 standard stars in the cluster field are $12.7 < V < 19.1$ and $0.4 < (B-V) < 1.9$ mag, respectively.

Table 1. Log of observations

Date	Object	X	Exposure time, s B, V, R_c, I_c
Aug. 27, 2003	NGC 7788	1.05	300, 300, 300, 300
			60, 30, 30, 30
	NGC 7790	1.07	300, 100, 100, 100
Aug. 29, 2003	NGC 7296	1.01	300, 300, 300, 300
			300, 300, 300, 300
			30, 30, 15, 15
	NGC 7790	1.06	300, 100, 100, 100
Oct. 15, 2009	NGC 7790	1.06	300, 150, 150, 150
	King 12	1.05	300, 300, 300, 300
			30, 30, 30, 30
	NGC 7788	1.05	300, 300, 300, 300
			−−, 30, 30, 30
	NGC 7790	1.06	300, 150, 150, 150
	NGC 7790	1.09	300, 150, 150, 150
Oct. 16, 2009	NGC 6940	1.05	300, 150, 150, 150
	Berkeley 96	1.05	300, 300, 300, 300
			30, 30, 30, 30
	Berkeley 97	1.04	300, 300, 300, 300
			30, 30, 30, 30
	NGC 7790	1.05	300, 150, 150, 150
	NGC 7296	1.06	300, 300, 300, 300
			30, 30, 30, 30
	NGC 7790	1.05	300, 150, 150, 150
	NGC 7790	1.09	300, 150, 150, 150
	NGC 7790	1.10	300, 150, 150, 150
Oct. 18, 2009	NGC 7790	1.06	300, 150, 150, 150
	Berkeley 97	1.06	300, 300, 300, 300
	NGC 7790	1.05	300, 150, 150, 150
	King 12	1.07	300, 300, 300, 300
	NGC 7790	1.08	300, 150, 150, 150
Oct. 19, 2009	NGC 7790	1.05	300, 150, 150, 150
	NGC 7790	1.10	300, 150, 150, 150
Nov. 18, 2009	NGC 7790	1.05	300, 150, 150, 150
	Berkeley 97	1.06	400, 400, −−, −−
	Berkeley 97	1.06	400, 400, −−, −−
	Berkeley 96	1.09	300, 300, 300, −−
		1.12	30, 30, 30, 30
	NGC 7790	1.07	300, 150, 150, 150

We used the following formulae (Hardie 1964) to transform the magnitudes and colours from the instrumental to the standard system:

$$V = v + \varepsilon(B-V) + \xi_{V_1},$$

$$V = v + \rho(V-R_c) + \xi_{V_2},$$

$$(B-V) = \mu(b-v) + \xi_{(B-V)},$$

$$(V-R_c) = \psi(v-r) + \xi_{(V-R_c)},$$

[2] http://http://www3.cadc-ccda.hia-iha.nrc-cnrc.gc.ca/community/STETSON/sta

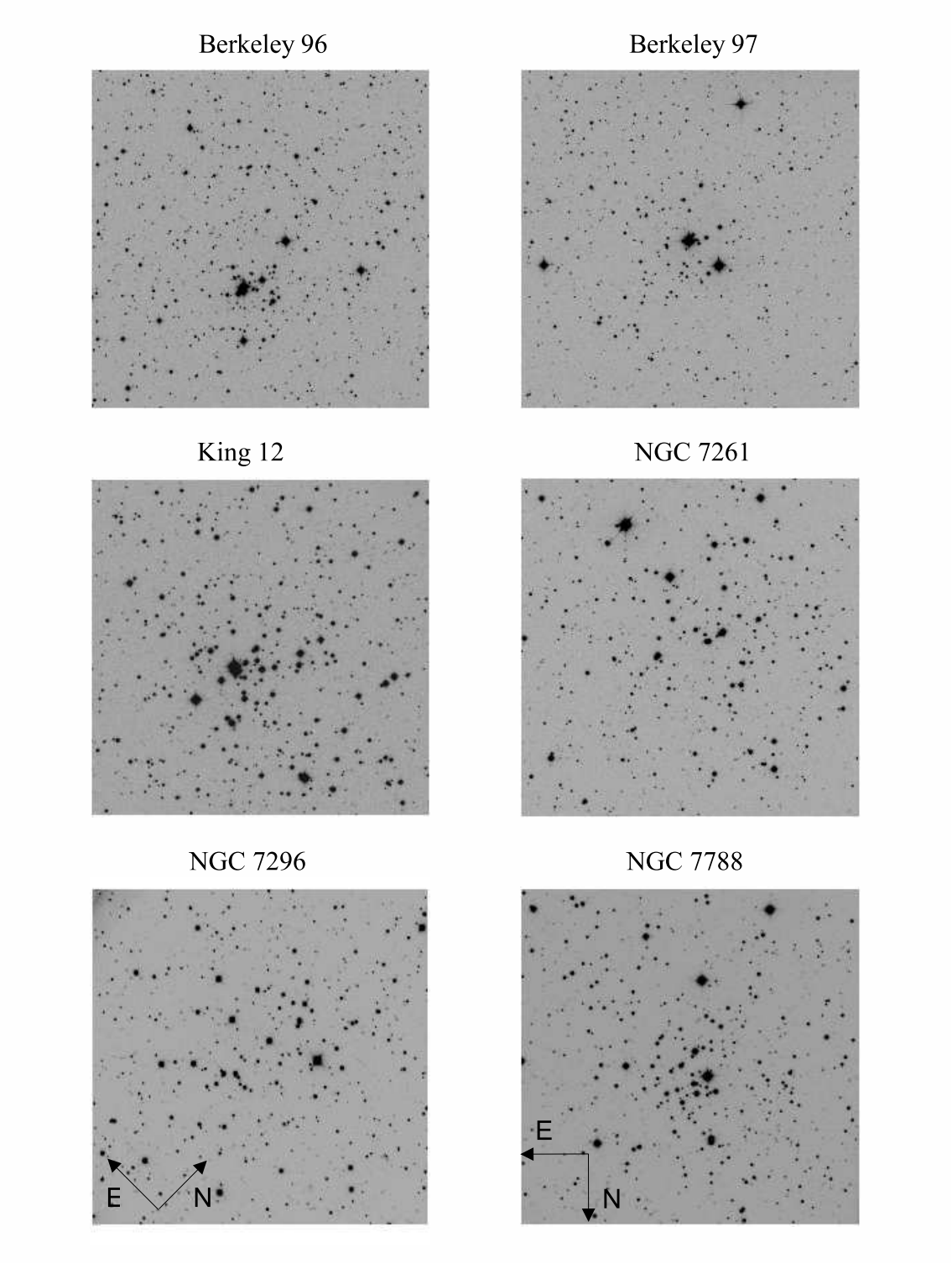

Figure 1. V–band images of the clusters studied (exposure time 300 s). The common orientation of all frames (except for NGC 7296) relative to the equatorial coordinate system is indicated by the arrows on the image of NGC 7788. The image size is near $8'\times 8'$ ($7'\times 7'$ for NGC 7296).

$$(V - I_c) = \varphi(v - i) + \xi_{(V-I_c)},$$

where b, v, r, and i are the magnitudes in the instrumental system and B, V, R_c, and I_c are the magnitudes in the standard system. The formula for the V magnitude as a function of $(V - R_c)$ colour was used only for the stars without B magnitudes. The averages of the median coefficients were $\varepsilon = -0.073 \pm 0.005$, $\rho = -0.125 \pm 0.012$, $\mu = 1.211 \pm 0.010$, $\psi = 0.803 \pm 0.010$, and $\varphi = 0.875 \pm 0.007$ for the observations done in 2003 and $\varepsilon = -0.076 \pm 0.003$, $\rho = -0.131 \pm 0.005$,

$\mu = 1.208 \pm 0.006$, $\psi = 0.910 \pm 0.006$, and $\varphi = 0.877 \pm 0.003$ for the observations done in 2009 (the *rms* deviations are given as the errors). We used mean values to recalculate the zero points ξ_{V_1}, ξ_{V_2}, $\xi_{(B-V)}$, $\xi_{(V-R_c)}$, and $\xi_{(V-I_c)}$ for the times of observations of the standard clusters. The differences in the ψ coefficients are presumably due to the changes in the photometer layout mentioned above.

As shown in Table 1, the standard clusters NGC 7790 and NGC 6940, and all program clusters were observed at the same air mass X. This explains why we did not estimate the extinction coefficients. In the cases where NGC 7790 was observed twice, before and after the program cluster, we calculated the zero points of the transformation expressions by a linear interpolation between zero point values calculated from the standard cluster. Weighted mean V magnitudes and $(B-V)$, $(V-R_c)$, and $(V-I_c)$ colours were computed and published only for those stars in the fields of the six program clusters, for which the magnitudes and colours derived from different frames and reduced to the standard system differ by less than 0.1 mag. This value (0.1 mag) seems to be the typical magnitude error for the faintest measured stars and, at the same time, close to 3σ-variance of magnitudes measured on different frames. The final values of the errors in the magnitudes and colours were calculated as the *rms* errors of the weighted mean on all frames (taking into account the errors in the aperture corrections and the errors introduced by the transformation from the instrumental system to the standard one). However, if the *rms* deviation of the magnitude or colour calculated on all frames exceeded the *rms* error of the weighted mean, this *rms* deviation was taken as the final error.

The results of the photometric study of the clusters Berkeley 96, Berkeley 97, King 12, NGC 7261, NGC 7296, and NGC 7788 are presented in Tables 4, 5, 6, 7, 8, and 9, respectively. Tables 4–9 are available in the electronic form only and are accessible at the CDS website [3] and at the Sternberg Astronomical Institute website [4]. In this paper, we list a sample of few lines of Table 4 only as an example. Tables 5–9 have the same layout. The tables include the equatorial coordinates α and δ in degrees at the epoch J2000, V magnitudes and $(B-V)$, $(V-R_c)$, and $(V-I_c)$ colours and their errors σ_V, $\sigma_{(B-V)}$, $\sigma_{(V-R_c)}$, and $\sigma_{(V-I_c)}$ for individual stars. We used 99.999 in all cells where the corresponding values are not available.

3 RESULTS AND DISCUSSION

3.1 Determination of Physical Parameters

We derived V magnitudes and $(B-V)$, $(V-R_c)$, and $(V-I_c)$ colours for the stars in the fields of Berkeley 96, Berkeley 97, King 12, NGC 7261, NGC 7296, and NGC 7788. In Fig. 2, the error in the magnitude, σ_V , and the errors in the colours, $\sigma_{(B-V)}$, $\sigma_{(V-R_c)}$, and $\sigma_{(V-I_c)}$, are plotted against the V magnitude for each cluster; the numbers on each plot indicate the number of stars. In most cases, the errors do not exceed 0.10 mag; the magnitude limit is 20-21.5 mag, depending on the band. The colour plots for NGC 7261 show narrow "tails", because only one frame in each band was taken with the exposure 300 s, and no averaging was performed; the same is seen for $\sigma_{(V-I_c)}$ (Berkeley 96).

We compared the derived magnitudes and colours with published photometry and show the magnitude and colour differences in Fig. 3. Our photometric data are in good agreement with all other photoelectric data - see plots for Be 96 and King 12, "star" symbols on the plots for NGC 7261 and NGC 7788. In contrast, the comparison of our CCD photometry with photographic values reported elsewhere exhibits rather wide spread, as shown by the "dot" symbols on the plots for NGC 7261 and NGC 7788. We also found systematic differences of approximately 0.2 ± 0.05 mag in V and 0.1 ± 0.05 mag in $(V-R_c)$ between our values and those derived by Netopil et al. (2005) for NGC 7296. Differences in the $(B-V)$ colours show the systematic trend from 0.1 to 0.25 mag. However, 32 common stars identified in the APASS catalogue show small negative differences of about -0.07 ± 0.03 mag in V and -0.04 ± 0.02 mag in $(B-V)$, respectively.

To estimate the cluster distance, age, and colour excess toward the cluster, we built the following colour–magnitude diagrams (CMD) for each program cluster: $(V, B-V)$, $(V, V-R_c)$, and $(V, V-I_c)$ – from our data, and $(J, J-H)$, $(K_s, J-K_s)$ – from the 2MASS catalogue. The faint stars with colour errors exceeding 0.05 mag were excluded from our consideration. We then fit each CMD to a solar-metallicity isochrone by Girardi et al. (2002) using the method developed by Koposov et al. (2008). In this method we superimposed the isochrone on the colour–magnitude diagram in such a way that the corresponding plot for the radial density distribution exhibits a peak for the stars lying in the vicinity of the isochrone (the distance in the colour index for such stars is less than 0.05 mag) and an almost flat distribution for all other stars (supposed field stars). The centers of clusters were found from density maps built using data from the 2MASS PSC. We considered the position of the maximum of the density peak as the center of the cluster, and the distance from the cluster center, at which the star density in the cluster region becomes flat on the radial density distribution and equal to the density of field stars, as the cluster radius. In this way we evaluated the distance, colour excess, and age for each cluster on each CMD. To convert the colour excesses found from different colour–magnitude diagrams to the colour excess $E(B-V)$ and to calculate the distance modulus, we used the following relations: $A_{K_s} = 0.670 \cdot E(J-K_s)$ (Dutra et al. (2002)) and $A_V = 3.08 \cdot E(B-V)$, $E(V-R_c) = 0.61 \cdot E(B-V)$, $E(V-I_c) = 1.35 \cdot E(B-V)$, $E(V-J) = 2.25 \cdot E(B-V)$, and $E(V-H) = 2.57 \cdot E(B-V)$ (He et al. (1995)).

Figures 4-9 present the $V-(B-V)$, $V-(V-R_c)$, $V-(V-I_c)$ (or $R-(R-I_c)$, see explanations below), and $J-(J-H)$ colour–magnitude diagrams, on which the corresponding isochrones are plotted (solid lines).

For each cluster, Table 2 gives the refined coordinates of the center, α_{J2000} and δ_{J2000}, the cluster diameter d in arcminutes, the age t in Myr, the colour excesses $E(B-V)$, and the true distance moduli $(m-M)_0$ determined from each CMD and recalculated using the relations above. On the whole, the parameters derived from different colour–magnitude diagrams agree well, although for some clusters we can see small differences in $E(B-V)$ values estimated

[3] http://cdsarc.u-strasbg.fr/
[4] http://ocl.sai.msu.ru/

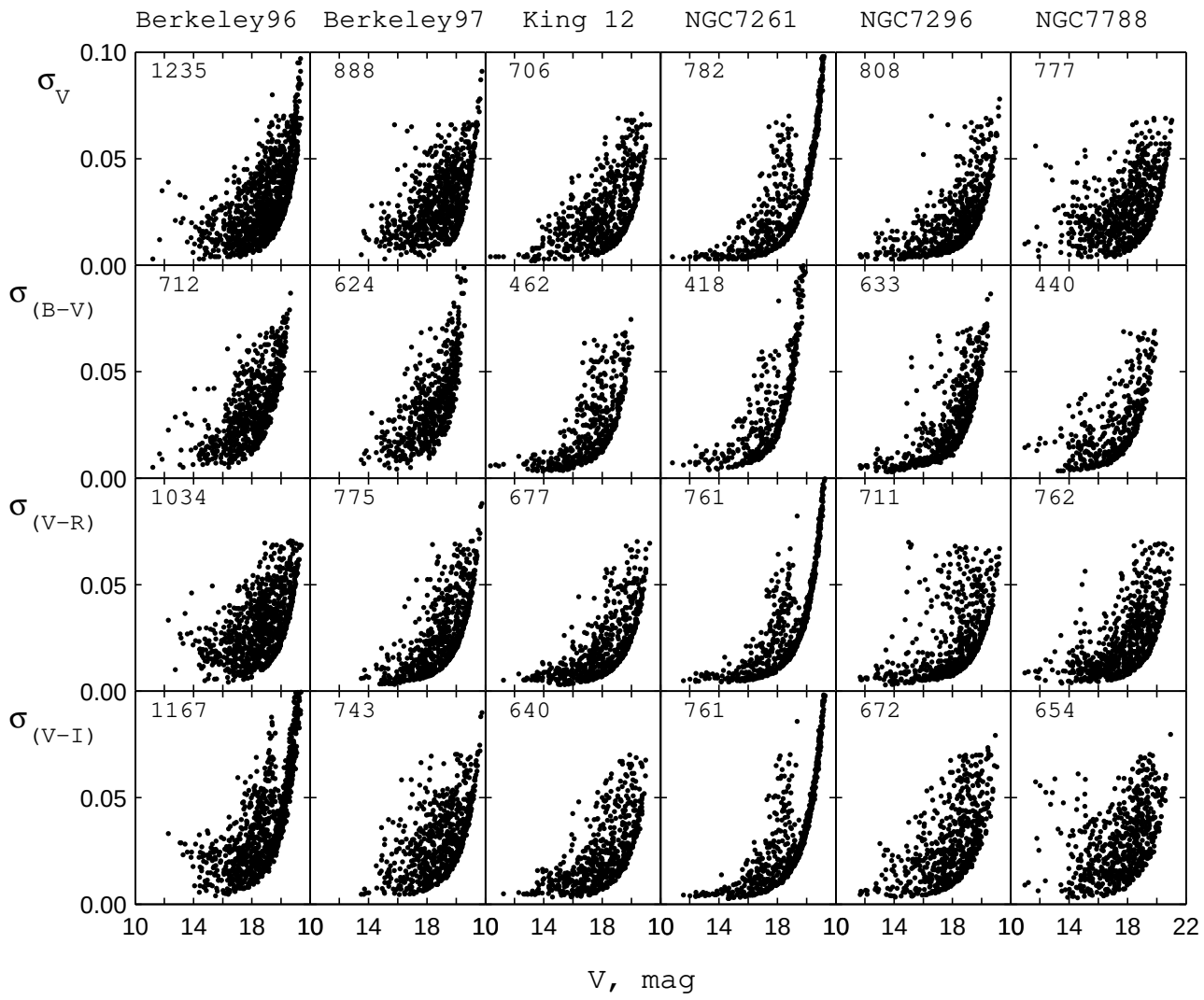

Figure 2. Errors in the magnitudes, σ_V , and in the colours, $\sigma_{(B-V)}$, $\sigma_{(V-R_c)}$, and $\sigma_{(V-I_c)}$, versus V magnitude for the program clusters (from left to right) Berkeley 96, Berkeley 97, King 12, NGC 7261, NGC 7296, and NGC 7788; the numbers on top of each plot indicate the number of stars; all values along the horizontal and vertical axes are given in magnitudes.

separately from optical and infrared data. We suppose that these differences can be due to greater contamination of the infrared CMDs by field stars as compared to optical data, and to the uncertainties of color excess transformations used. The final values of mean colour excesses and the true distance moduli, along with their *rms* deviations, are listed in Table 3. All CMDs yield approximately the same age estimates for each cluster, so we did not put any errors for the ages, which generally depend on the isochrones used. We could not derive the cluster parameters from the $(K_s, J-K_s)$ diagram for NGC 7788, because of the large dispersion of stars in this CMD.

Let us compare our parameters with those from the literature. Table 3 contains the colour excesses $E(B-V)$, true distance moduli $(m-M)_0$, distances r in parsecs, and logarithms of the age *lgt* from this paper and different published sources. For the clusters King 12, NGC 7261, and NGC 7788, we include data from both Loktin et al. (2001) and Dias et al. (2002), because Loktin et al. (2001) determined the distance moduli, and Dias et al. (2002) included these distances in his catalogue. Table 3 shows that only in the case of the King 12 cluster our parameters are in good agreement with those obtained in the previous study by Mohan & Pandey (1984). For the remaining five clusters investigated in this study, the physical parameters have been considerably improved.

3.2 Mass Function

For three clusters – Berkeley 97, King 12, and NGC 7788 – we noticed gaps on their main sequences on all CMDs built from our BVR_cI_c CCD photometry. To verify these gaps, we extracted r and i data from the IPHAS survey (Drew et al. (2005)) and transformed these values from the

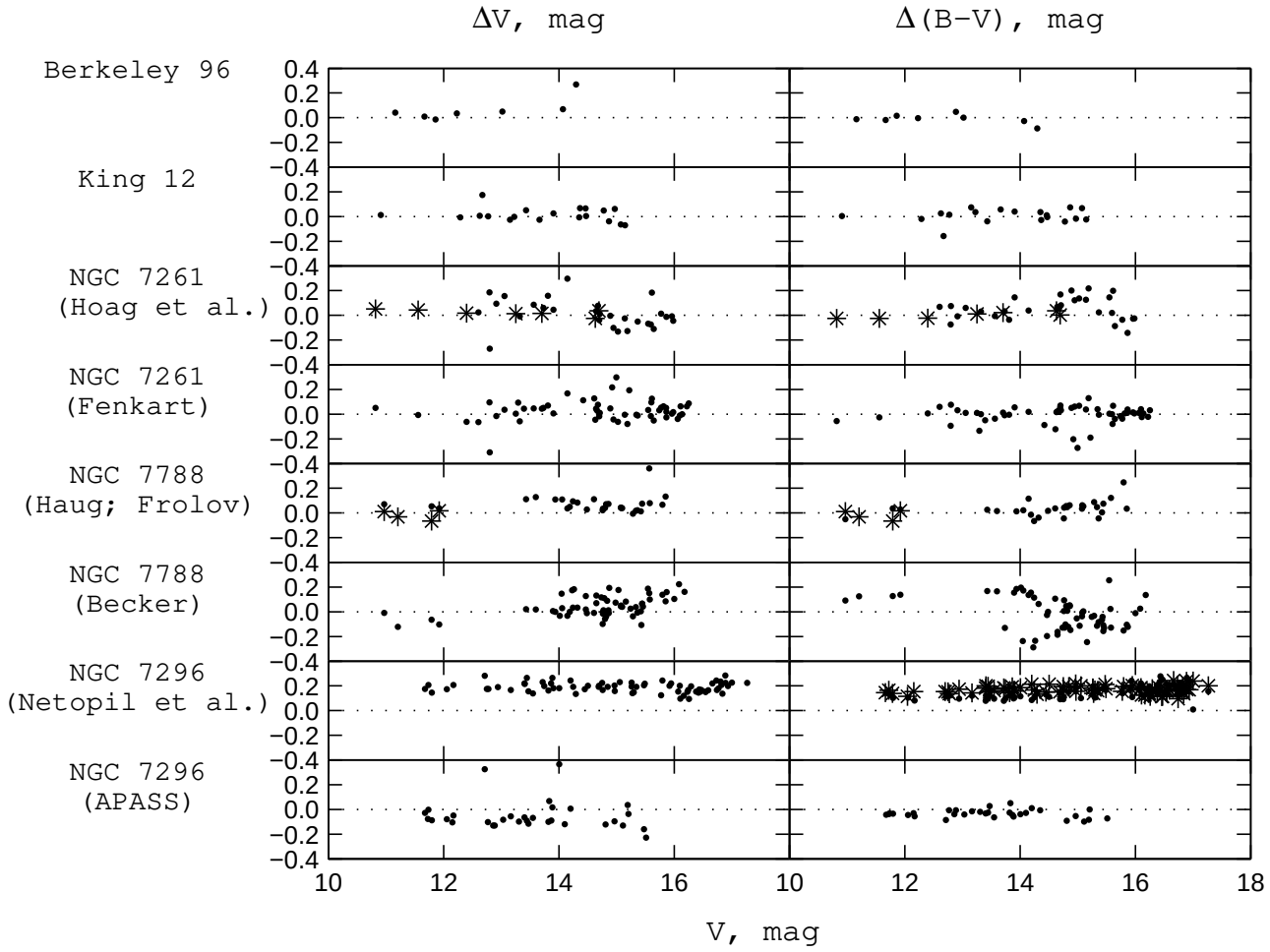

Figure 3. Differences of magnitudes, ΔV (left), and colours, $\Delta(B-V)$ (right), for common stars in this paper and Del Rio (1984) in the field of Berkeley 96; in this paper and Mohan & Pandey (1984) in the field of King 12; in this paper and Hoag et al. (1961) (symbol "star" – photoelectric photometry, symbol "dot" – photographic photometry), Fenkart (1968) in the field of NGC 7261; in this paper and Haug (1970) (symbol "star"), Frolov (1977) (symbol "dot"), Becker (1965) in the field of NGC 7788; in this paper and Netopil et al. (2005) (symbol "star" – $\Delta(B-V)$, symbol "dot" – $\Delta(V-R)$) in the field of NGC 7296; in this paper and the APASS catalogue in the field of NGC 7296. The V magnitude is along the horizontal axis on all plots; the dashed line corresponds to zero magnitude and colour differences.

SDSS system into Cousins R, I magnitudes using empirical colour transformations by Jordi et al. (2006). We then built colour–magnitude diagrams $(R, R-I_c)$ using both our photometric data and those derived from IPHAS. Figures 5, 6, and 9 include these two CMDs. For each cluster, the gap on the main sequence is situated at the same values of magnitudes and colours on both diagrams – $(R, R-I_c)$ and $(R_{iphas}, (R-I)_{iphas})$. We used solar-metallicity evolutionary tracks and isochrones by Girardi et al. (2002) to evaluate the mass intervals (in solar-mass units) that correspond to these MS gaps: [1.3–1.5] for Berkeley 97, [1.4–1.6] for King 12, and [1.5–1.7] for NGC 7788.

Present-day luminosity and mass functions for these three clusters were built by star counts for all stars fainter than those at the MS turn-off. To evaluate the completeness of our photometric data, we used the method described by Sagar & Richtler (1991). Artificial stars were added to our initial images in the B and I_c filters. The fraction of artificial stars (most of them are faint) does not exceed 10% of the total population. Images with artificial stars are then processed using the same algorithm. The portion of restored stars in each interval of magnitudes gives us the completeness value in the same magnitude intervals. We used the least of the two values obtained by V and I_c images according to Sagar & Richtler (1991). This method makes it possible to find the real PDLF with errors less than 3% in each magnitude interval where the completeness is more than 0.5. The members of each cluster were selected by photometric criteria using $(V, V-I_c)$ diagrams. We built the PDLF for stars inside the cluster radius and for the field stars, and corrected both functions for the incompleteness factor and for the area difference. The resulting PDLF is the difference between the cluster PDLF and the field stars PDLF.

To convert the luminosity function into the mass function, we used stellar evolutionary tracks and solar-metallicity isochrones by Girardi et al. (2002). Fig-

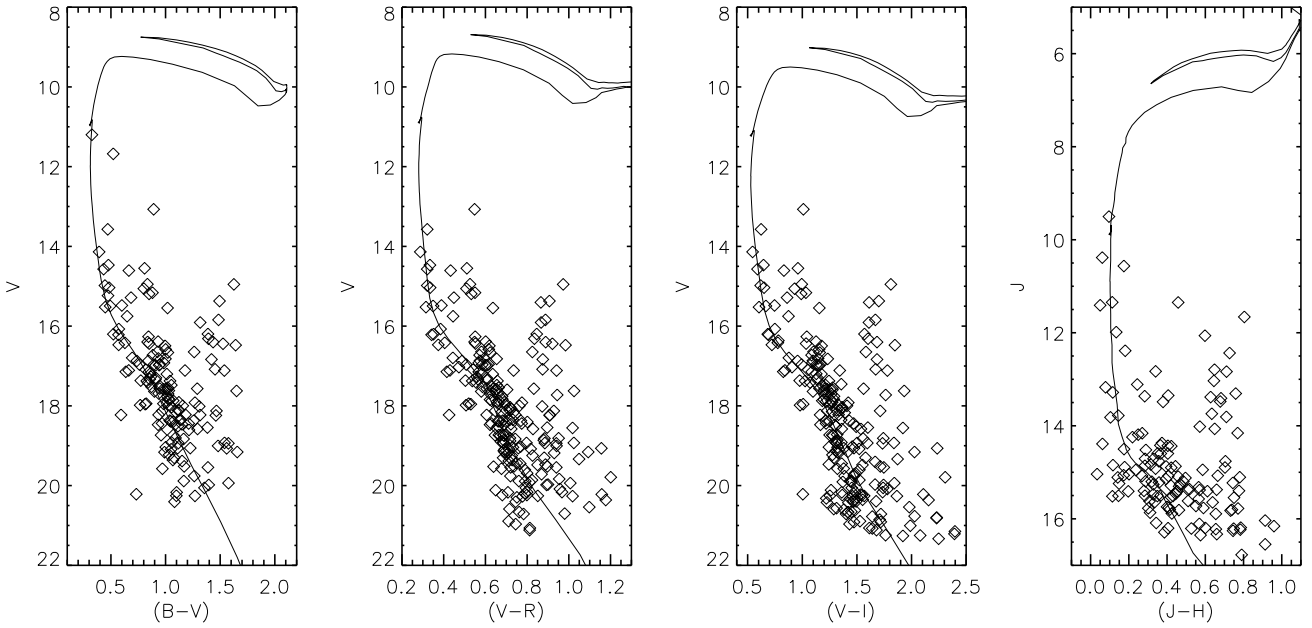

Figure 4. Colour–magnitude diagrams for Berkeley 96. The diamonds mark the positions of stars on the diagram; the solid lines indicate the corresponding isochrones. All values along the horizontal and vertical axes are given in magnitudes. The size of the region for which the diagram was constructed is 3′.

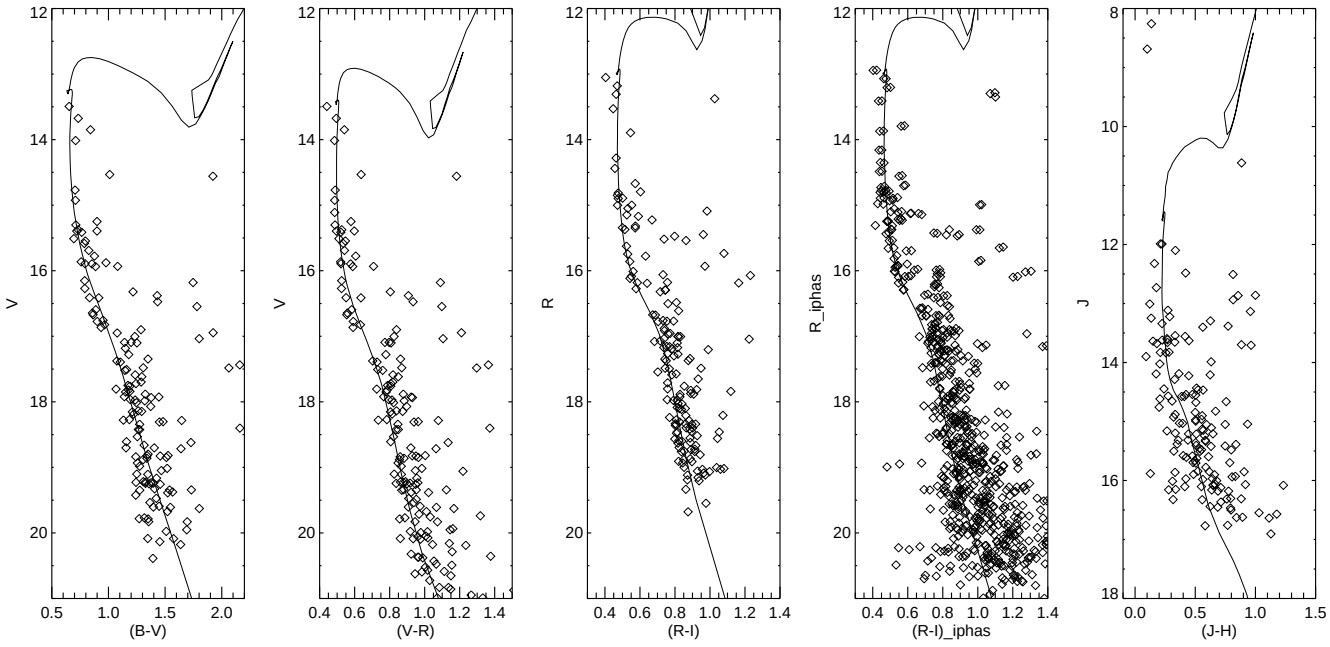

Figure 5. Colour–magnitude diagrams for Berkeley 97. The diamonds mark the positions of stars on the diagram; the solid lines indicate the corresponding isochrones. All values along the horizontal and vertical axes are given in magnitudes. The size of the region for which the diagram was constructed is 4′.

ures 10, 11, and 12 show the MFs for clusters Berkeley 97, King 12, and NGC 7788. The values of the power law exponent (logarithmic mass function slope) – α was calculated by the χ^2 solution for linear regression without taking into account escape points in the case of King 12 and NGC 7788. The gaps on each plot are plotted according to main sequence gaps on the colour-magnitude diagrams. The escape point on Fig. 11 and Fig. 12 corresponds to the deficiency or the absence of stars in the gaps. There is no such point on Fig. 10 although a main sequence gap can be clearly seen in

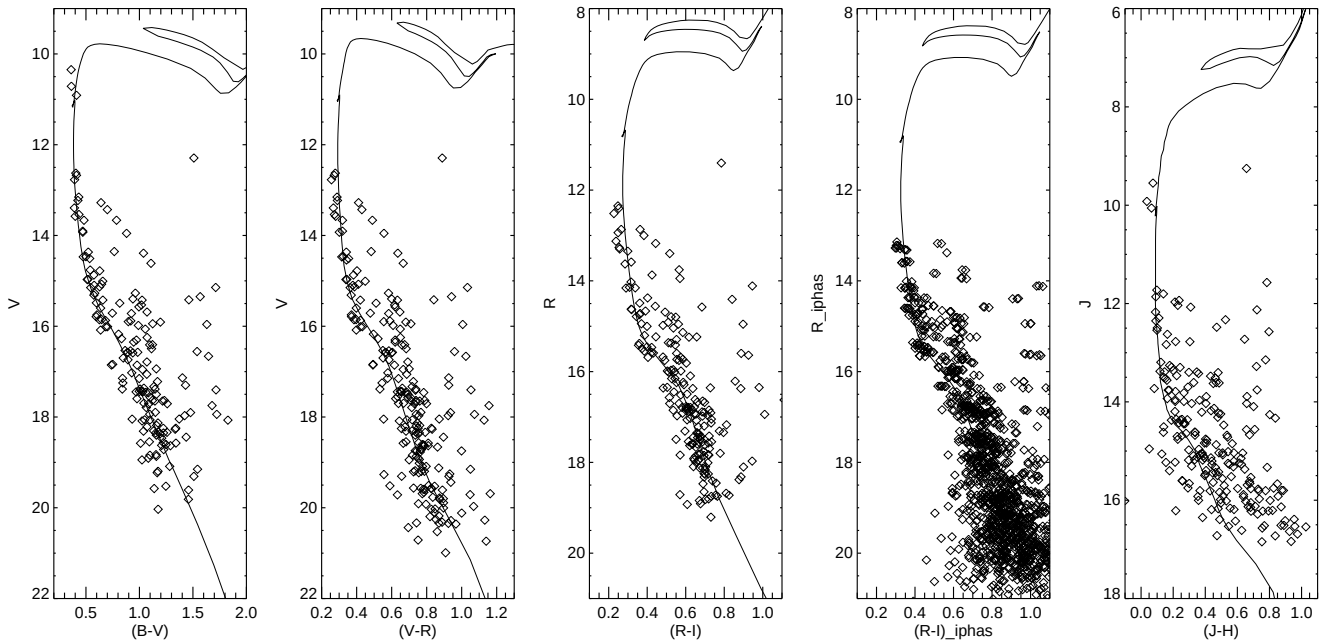

Figure 6. Colour–magnitude diagrams for King 12. The diamonds mark the positions of stars on the diagram; the solid lines indicate the corresponding isochrones. All values along the horizontal and vertical axes are given in magnitudes. The size of the region for which the diagram was constructed is 5′.

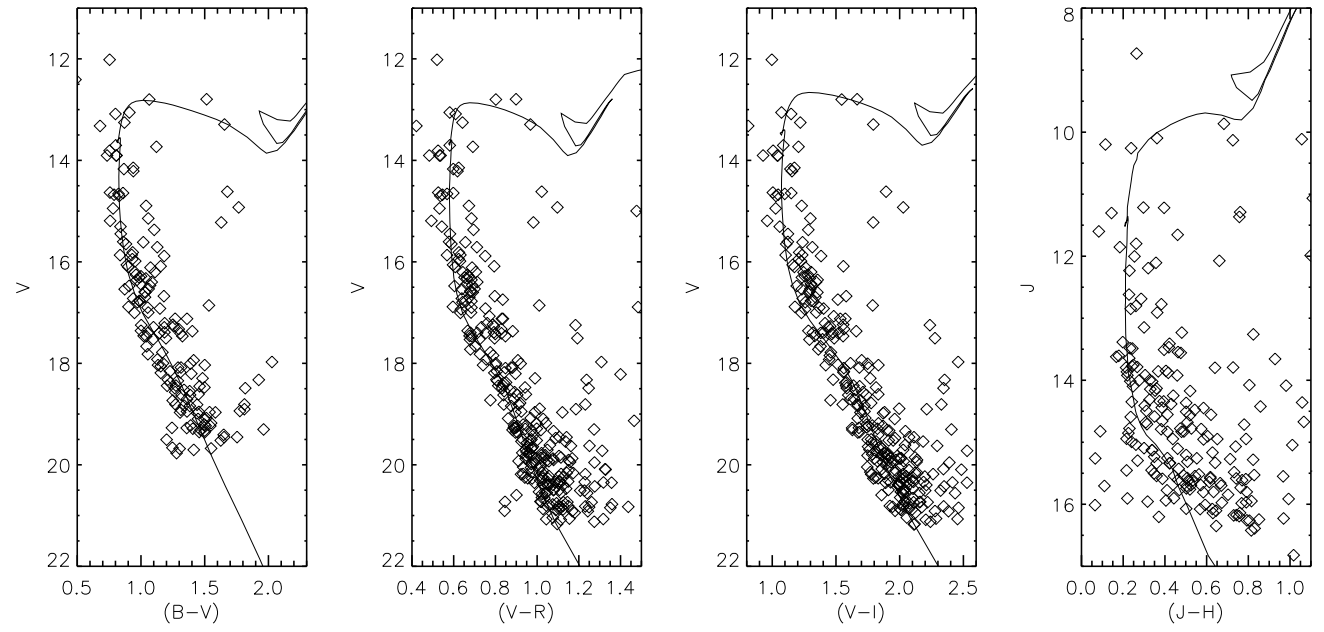

Figure 7. Colour–magnitude diagrams for NGC 7261. The diamonds mark the positions of stars on the diagram; the solid lines indicate the corresponding isochrones. All values along the horizontal and vertical axes are given in magnitudes. The size of the region for which the diagram was constructed is 7′.

the case of Berkeley 97. It can be explained by the insufficient subtraction of field stars. Such gaps and breaks in MF plots may be due to a discontinuity in the process of star formation inside the cluster.

4 CONCLUSIONS

We used our optical BVR_cI_c CCD observations to obtain the V magnitudes and $(B-V)$, $(V-R_c)$, and $(V-I_c)$ colours for a large number of stars in the fields of six open clusters: Berkeley 96, Berkeley 97, King 12, NGC 7261, NGC 7296,

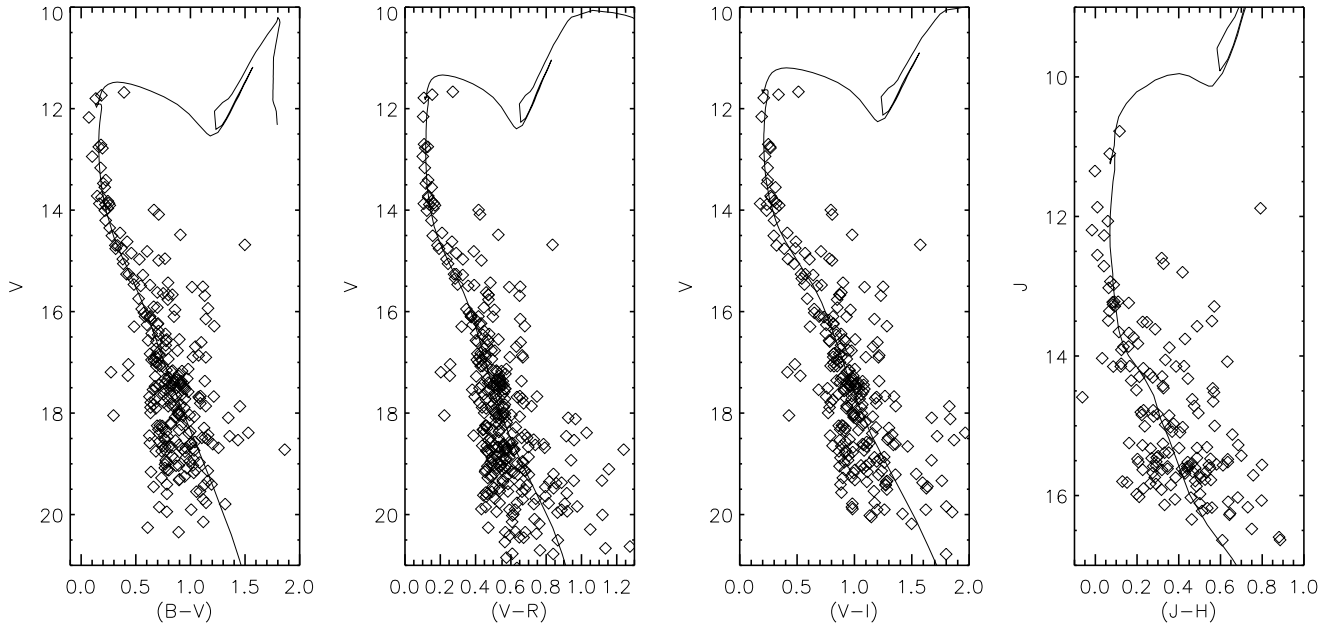

Figure 8. Colour–magnitude diagrams for NGC 7296. The diamonds mark the positions of stars on the diagram; the solid lines indicate the corresponding isochrones. All values along the horizontal and vertical axes are given in magnitudes. The size of the region for which the diagram was constructed is 8′.

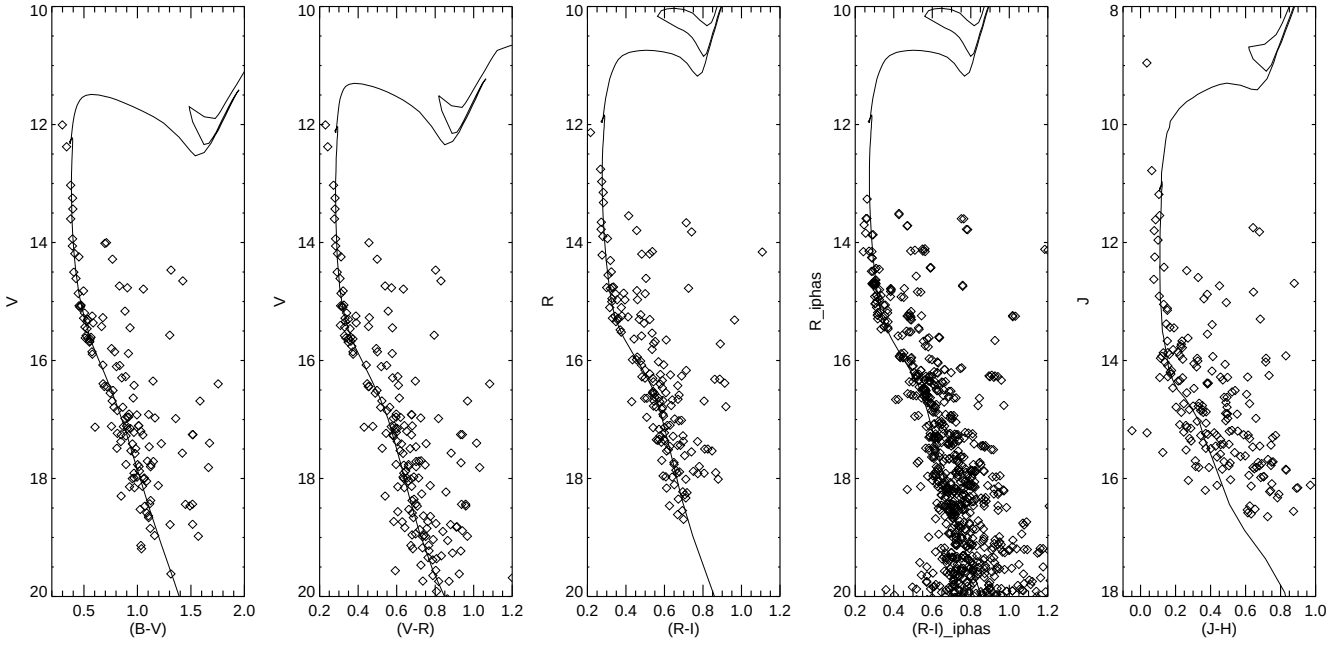

Figure 9. Colour–magnitude diagrams for NGC 7788. The diamonds mark the positions of stars on the diagram; the solid lines indicate the corresponding isochrones. All values along the horizontal and vertical axes are given in magnitudes. The size of the region for which the diagram was constructed is 4′.

and NGC 7788 (see electronic Tables 4-9). For each cluster, we constructed optical and infrared (based on 2MASS data) colour–magnitude diagrams with the Padova isochrones superimposed (Figs. 4-9). We used this technique to derive the ages, distances, and colour excesses of the clusters under study (Table 3).

We found three clusters – Berkeley 97, King 12, and NGC 7788 – to have gaps on their main sequences. Independent data extracted from the IPHAS (Drew et al. (2005))

Table 2. Cluster parameters determined from optical and infrared data

	Berkeley 96	Berkeley 97	King 12	NGC 7261	NGC 7296	NGC 7788
α_{J2000}	$22^h29^m49^s$	$22^h39^m28^s$	$23^h53^m01^s$	$22^h20^m07^s$	$22^h28^m01^s$	$23^h56^m38^s$
δ_{J2000}	$+55°23'47''$	$+58°59'51''$	$+61°56'45''$	$+58°07'41''$	$+52°19'22''$	$+61°24'02''$
d	$3'$	$4'$	$5'$	$7'$	$8'$	$4'$
t, Myr	40	250	70	160	280	160
			$E(B-V)$, mag			
$V, B-V$	0.50	0.72	0.54	1.00	0.22	0.49
$V, V-R_c$	0.58	0.85	0.57	0.93	0.24	0.52
$V, V-I_c$	0.53	0.75	0.51	0.86	0.19	0.49
$J, J-H$	0.55	0.79	0.47	0.78	0.28	0.47
$K_s, J-K_s$	0.56	0.72	0.44	0.83	0.25	−−
			$(m-M)_0$, mag			
$V, B-V$	12.71	12.08	12.05	12.16	12.18	12.39
$V, V-R_c$	12.39	11.86	11.83	12.35	11.97	12.09
$V, V-I_c$	12.89	12.13	12.19	12.41	11.98	12.30
$J, J-H$	12.23	11.76	11.96	12.16	11.72	12.03
$K_s, J-K_s$	12.31	11.71	11.85	12.21	11.92	−−

Table 3. Comparison of our cluster parameters with published data

	$E(B-V)$, mag	$(m-M)_0$, mag	r, pc	$\lg t$	Source
Berkeley 96	0.54 ± 0.03	12.51 ± 0.28	3180^{+440}_{-380}	7.60	this paper
	0.68	13.61	5300		Del Rio (1984)
Berkeley 97	0.77 ± 0.06	11.91 ± 0.19	2410^{+220}_{-200}	8.40	this paper
	0.75	11.28	1800 ± 85	7.30	Tadross (2008)
King 12	0.51 ± 0.05	11.98 ± 0.15	2490^{+180}_{-170}	7.85	this paper
	$0.52 - 0.69$	11.98	2490 ± 85		Mohan & Pandey (1984)
	0.59	12.034		7.037	Loktin et al. (2001)
	0.59		2378	7.037	Dias et al. (2002)
	0.59	11.88		7.12	Kharchenko et al. (2005)
NGC 7261	0.88 ± 0.09	12.26 ± 0.12	2830^{+160}_{-150}	8.20	this paper
	0.48	11.7	2200	8.3	Jennens & Helfer (1975)
	1.00	12.55	3230	7.0	Fenkart (1968)
	0.969	11.280		7.670	Loktin et al. (2001)
	0.969		1681	7.670	Dias et al. (2002)
NGC 7296	0.24 ± 0.03	11.95 ± 0.16	2450^{+190}_{-170}	8.45	this paper
	0.15 ± 0.02	12.33 ± 0.2	2930 ± 350	8.0 ± 0.1	Netopil et al. (2005)
NGC 7788	0.49 ± 0.02	12.20 ± 0.17	2750^{+220}_{-210}	8.20	this paper
	0.283	12.030		7.593	Loktin et al. (2001)
	0.283		2374	7.593	Dias et al. (2002)
	0.48	11.87		7.48	Kharchenko et al. (2005)

catalogue confirmed these features on colour-magnitude diagrams for these three clusters. We built the luminosity function and the mass function for these clusters and found the features on the MF plot.

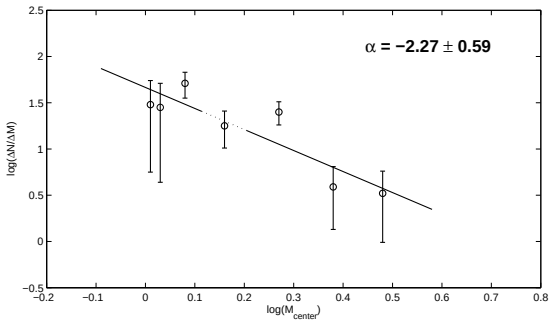

Figure 10. Mass function of Berkeley 97.

ACKNOWLEDGMENTS

We used the WEBDA database operated at the Institute for Astronomy of the University of Vienna and developed by E. Paunzen and J.-C. Mermilliod; 2MASS data, which is a joint project of the University of Massachusetts and the Infrared Processing and Analysis Center/California Institute of Technology, funded by NASA and NSF; the APASS database, located at the AAVSO website [5]; and the Virtual observatory resource [6] developed at Sternberg Astronomical Institute

[5] http://www.aavso.org/apass

[6] http://vo.astronet.ru

Table 4. Photometric data for Berkeley 96

α_{J2000}, deg	δ_{J2000}, deg	V	σ_V	$B-V$	$\sigma_{(B-V)}$	$V-R_c$	$\sigma_{(V-R_c)}$	$V-I_c$	$\sigma_{(V-I_c)}$
337.446900	55.392340	11.200	0.003	0.326	0.005	99.999	99.999	99.999	99.999
337.567690	55.446010	16.511	0.027	0.806	0.014	0.525	0.026	0.990	0.024
337.378080	55.451410	18.611	0.028	1.145	0.062	0.722	0.036	1.314	0.040
337.374210	55.451490	19.292	0.023	1.394	0.036	0.926	0.016	1.720	0.049
...	...	...	...	...	...	...	...	...	...

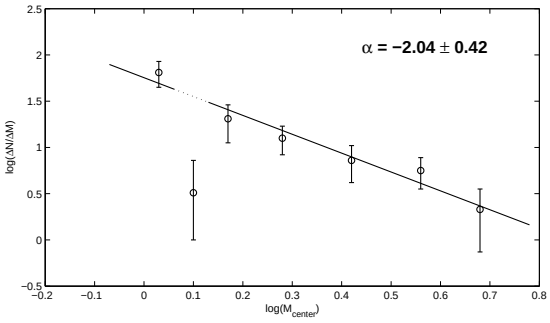

Figure 11. Mass function of King 12.

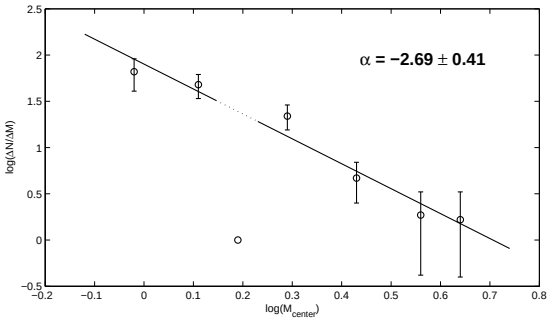

Figure 12. Mass function of NGC 7788.

(Moscow State University). We thank L.N. Berdnikov, O.V. Vozyakova, and A.K. Dambis for valuable advice and the anonymous referee for useful comments.

REFERENCES

Becker W., 1965, Mem. Soc. Astron. Italiana, 36, 277
Dias W.S., Alessi B.S., Moitinho A. and Lepine J.R.D., 2002, A&A, 389, 871 [7]
Drew J.E., Greimel R., Irwin M.J., et al. 2005, MNRAS, 362, 753
Dutra C.M., Santiago B.X. and Bica E., 2002, A&A, 381, 219
Eggen O.J., 1968, Royal Obs. Bull., No. 137
Fenkart R.P., 1968, Mem. Soc. Astron. Italiana, 39, 85
Frolov V.N., 1977, Izv. Glavn. Astron. Obs. Pulkovo, 195, 80
Girardi L., Bertelli G., Bressan A., et al., 2002, A&A, 391, 195
Glushkova E.V., Zabolotskikh M.V., Koposov S.E. et al., 2010, Astronomy Letters, 36, 14
Hardie R.H., 1964, Photoelectric Reductions in the book Astronomical Techniques, ed.W. A. Hiltner, University of Chicago, p. 178.
Haug U., 1970, A&AS, 1, 35
He L., Whittet D.C.B., Kilkenny D, and Spencer Jones J.H., 1995, A&AS, 101, 335
Hoag A.A., Johnson H.L., Iriarte B., et al., 1961, Publ. US. Nav. Obs., 17, 345
Jennens P.A., Helfer H.L., 1975, MNRAS, 172, 681
Jordi K., Grebel E.K. and Ammon A., 2006, A&A, 460, 339
Kharchenko N.V., Piskunov A.E., Roser S. et al., 2005, A&A, 438, 1163
Koposov S.E., Glushkova E.V. and Zolotukhin I.Yu., 2008, A&A, 486, 771
Kubinec W.R., 1973, Publ. Warner Swasey Obs., 1, No. 3
Loktin A.V., Gerasimenko T.P. and Malysheva L.K., 2001, Astron. Astrophys. Trans., 20, 607
Mohan V., Pandey A.K., 1984, Ap&SS, 105, 315
Netopil M., Paunzen E., Maitzen H.M., et al., 2005, Astron. Nachr., 326, 734
Del Rio G., 1984, A&AS, 56, 289
Sagar R., Richtler T., 1991, A&A, 250, 324
Skrutskie M.F., Cutri R.M., Stiening R., et al., 2006, AJ, 131, 1163
Stetson P.B., 1987, PASP, 99, 191
Tadross A.L., 2008, MNRAS, 389, 285

[7] www.astro.iag.usp.br/.wilton/clusters.txt (2012)